# A NOVEL TWO-DIMENSIONAL CONVECTION-DIFFERENCE FINITE-DIFFERENCE SCHEME

**Tony W. H. Sheu, C. F. Chen, W. S. Huang, and L. W. Hsieh**
*Department of Naval Architecture and Ocean Engineering, National Taiwan University, 73 Chou-Shan Rd., Taipei, Taiwan, Republic of China*

*In this article, we develop a two-dimensional finite-difference scheme for solving the convection-diffusion equation. The numerical method involves using transformation on the prototype scalar transport equation and transferring it to a Helmholtz equation. We apply the alternating-direction implicit scheme of Polezhaev to solve for the Helmholtz equation. As the key to success in simulating the convection-diffusion equation, we exploit the solution pertaining to the Helmholtz equation in the course of scheme development, thereby providing high-level accuracy to the prediction. Since this is a new method developed for solving the model equation, it is illuminating to conduct modified equation analysis on the discrete equation in order to make a full assessment of the proposed method. The results provide us with useful insights into the nature of the scheme. It is standard practice to validate the code by investigating test problems which are amenable to exact solutions to the working equation. Results show exact agreement for the one-dimensional test problem and good agreement with the analytic solutions for two-dimensional problems.*

## 1. INTRODUCTION

In this article, we develop a numerical method for solving the convection-diffusion scalar transport equation. This equation is encountered in a broad range of fluid dynamics and heat transfer applications. The model equation to be investigated is also academically important since it is regarded as the simplest prototype equation for modeling most of the transport phenomena. It is this practical as well as theoretical importance that makes numerical prediction of this model equation worthwhile and thus motivates the present study. We restrict our attention to two-dimensional cases in the $x$–$y$ plane.

A reliable transport scheme must have the ability to suppress numerical instabilities arising from convective terms. The problem of numerical instabilities of this sort is, in particular, severe when convective terms dominate diffusive terms in multiple dimensions [1]. The aim of the present article is to find a way to avoid dealing with these convective terms in the equation. One way to make progress

Address correspondence to Prof. Tony W. H. Sheu, Department of Naval Architecture and Ocean Engineering, National Taiwan University, 73 Chou-Shan Rd., Taipei, Taiwan, Republic of China. E-mail: sheu@indy.na.ntu.edu.tw

## NOMENCLATURE

| | | | |
|---|---|---|---|
| $c$ | coefficient of $\phi$ shown in Eq. (9) | $v$ | velocity component along the $y$ direction |
| $C(m)$ | cosine Fresnel integral $(= \sqrt{2/\pi} \int_0^m \cos n^2 \, dn)$ | $x, y$ | spatial coordinates |
| $f$ | source term shown in Eq. (9) | $\Gamma$ | source term shown in Eq. (1) |
| $h$ | mesh size | $\phi$ | auxiliary scalar defined in Eq. (4) |
| $k$ | diffusivity of the working fluid | | |
| $S(m)$ | sine Fresnel integral $(= \sqrt{2/\pi} \int_0^m \sin n^2 \, dn)$ | $\Phi$ | primary passive scalar |
| $u$ | velocity component along the $x$ direction | | |

is to apply a mapping by relating the original passive scalar to the other auxiliary scalar. The use of transformation as described in Section 2 transforms the original prototype equation into the Helmholtz equation, thereby avoiding convective terms which may cause solutions to diverge. It is, then, a question of constructing a scheme to solve for the Helmholtz equation, and this is another main theme of the present study. When solving the Helmholtz equation, we are concerned with prediction accuracy and computational efficiency since we do not regard a scheme as useful if it cannot provide accuracy at a certain high level.

The rest of this article is organized as follows. Section 2 presents the working equation. In Section 3, we transform the model equation into the Helmholtz equation, which is one of the main themes of this study. This is followed by presentation of the finite-difference scheme used to solve the Helmholtz equation in two dimensions. Our emphasis is on the application of the alternating-direction implicit scheme of Polezhaev [2]. In each iterative scheme, prediction of higher accuracy is our underlying goal to achieve. Section 4 is devoted to a fundamental study on the proposed flux discretization scheme, with an emphasis on modified equation analysis. Section 5 presents numerical results that demonstrate the validity of the method. In Section 6, we give concluding remarks.

## 2. WORKING EQUATION AND SOLUTION ALGORITHM

We consider in this article the following two-dimensional model equation for simulating the transport of a passive scalar $\Phi$ in the domain $\Omega$:

$$u\Phi_x + v\Phi_y - k(\Phi_{xx} + \Phi_{yy}) = -\Gamma \tag{1}$$

In the above, $\Gamma$ is the source term, $u$ and $v$ represent velocity components along the $x$ and $y$ directions, respectively, and $k$ denotes the diffusion coefficient. The above equation, subject to the Dirichlet-type boundary condition, $\Phi = g$ on $\partial\Omega$, constitutes a closure boundary-valued problem.

## 3. NUMERICAL MODEL

There are several ways to rectify numerical instabilities stemming from convective terms in transport equation (1). The strategy we will consider for overcoming this difficulty is described as follows. We first rewrite Eq. (1) as

$$\Phi_{xx} + \Phi_{yy} = 2A\Phi_x + 2B\Phi_y + F \tag{2}$$

where

$$A = \frac{u}{2k} \tag{3a}$$

$$B = \frac{v}{2k} \tag{3b}$$

$$F = \frac{\Gamma}{k} \tag{3c}$$

Unless otherwise stated, the subscript $p$ in $q_p$ denotes the derivative of $q$ with respect to $p$.

We can now proceed to transform Eq. (2) using a newly introduced passive scalar $\phi$, which relates the primary variable $\Phi$ through the mapping given by

$$\Phi = e^{Ax+By}\phi(x, y) \tag{4}$$

Our formulation involves substituting Eq. (4) into Eq. (2), thereby obtaining a partial differential equation for the transport of $\phi$ as follows:

$$\nabla^2\phi - K^2\phi = \bar{f} - 2C\phi_x - 2D\phi_y \tag{5}$$

where

$$K^2 = A^2 + B^2 - C^2 - D^2 - E \tag{6a}$$

$$C = A_x x + B_x y \tag{6b}$$

$$D = A_y x + B_y y \tag{6c}$$

$$E = A_{xx}x + 2A_x + B_{xx}y + A_{yy}x + 2B_y + B_{yy}y \tag{6d}$$

$$\bar{f} = \frac{F}{e^{Ax+By}} \tag{6e}$$

In what follows, velocities $u$ and $v$ and flow property of the fluid $k$ are assumed to be uniform throughout the domain of flow for purposes of illustration. When solving the resulting classical equation, we can apply the integral approach, which involves using Green's functions [3]. Unfortunately, computation of Green's functions is generally a difficult task; thus, they are seldom used in practice. As a result, we are led to consider conventional methods, such as the finite-difference method chosen for the present study. For purposes of computational efficiency in solving the multidimensional equation, we apply the alternating-direction implicit (ADI) scheme of Polezhaev [2] to solve Eq. (5). According to this operator-splitting strategy, calculation proceeds iteratively through two steps given below.

*Predictor step:*

$$-\phi^*_{xx} + K^2\phi^* = \phi^n_{yy} \tag{7}$$

*Corrector step:*

$$-\phi_{yy}^{n+1} + K^2\phi^{n+1} = \phi_{xx}^* \tag{8}$$

Taking a look at Eqs. (7)–(8), it becomes clear that the key to success in solving Eq. (1) lies in the calculation of the following model equation:

$$-k\phi_{xx} + c\phi = f \tag{9}$$

As is the case when a partial differential equation is solved, we aim to obtain a higher prediction accuracy for the model equation. Therefore, we employ the following general solution for the Eq. (9):

$$\phi = ae^{\lambda_1 x} + be^{\lambda_2 x} + \frac{f}{c} \tag{10}$$

In the above, $a$ and $b$ are constants. Substituting Eq. (10) into Eq. (9), we have two equations for $\lambda_1$ and $\lambda_2$, respectively:

$$k\lambda_1^2 - c = 0 \tag{11}$$

$$k\lambda_2^2 - c = 0 \tag{12}$$

The above two equations enable us to determine $\lambda_1$ and $\lambda_2$ as follows:

$$\lambda_1 = \sqrt{\frac{c}{k}} \tag{13a}$$

$$\lambda_2 = -\sqrt{\frac{c}{k}} \tag{13b}$$

We proceed to derive the discrete expression for Eq. (9) at an interior point $i$. Our strategy is to approximate derivative terms in Eq. (9) in a center-like form as follows:

$$-\frac{m}{h^2}(\phi_{i+1} - 2\phi_i + \phi_{i-1}) + \frac{c}{6}(\phi_{i-1} + 4\phi_i + \phi_{i+1}) = f \tag{14}$$

or

$$\left(-\frac{m}{h^2} + \frac{c}{6}\right)\phi_{i-1} + 2\left(\frac{m}{h^2} + \frac{c}{3}\right)\phi_i + \left(-\frac{m}{h^2} + \frac{c}{6}\right)\phi_{i+1} = f \tag{15}$$

In the above, $h$ is the uniform grid size. Given the above discrete representation of Eq. (9), the quality of prediction depends solely on $m$ shown in Eq. (14) or (15). As previously noted, we seek higher accuracy through use of the exact solutions evaluated at nodal points $i$ and $i\pm1$. By virtue of Eq. (10), we can substitute $\phi_i = ae^{\lambda_1 x_i} + be^{\lambda_2 x_i} + f/c$, $\phi_{i+1} = ae^{\lambda_1 h}e^{\lambda_1 x_i} + be^{\lambda_2 h}e^{\lambda_2 x_i} + f/c$, and $\phi_{i-1} = ae^{-\lambda_1 h}e^{\lambda_1 x_i} + be^{-\lambda_2 h}e^{\lambda_2 x_i} + f/c$ into Eq. (15) to derive

$$m = \frac{ch^2}{6} \cdot \frac{e^{\lambda_1 h} + e^{\lambda_2 h} + 4}{e^{\lambda_1 h} + e^{\lambda_2 h} - 2} \tag{16}$$

## 4.  MODIFIED EQUATION ANALYSIS

As the two-step iterative procedures terminate, the solution at the point $(i, j)$ is, in principle, obtained from the following five-point stencil equation:

$$a_{i,j+1}\phi_{i,j+1} + a_{i-1,j}\phi_{i-1,j} + a_{i,j}\phi_{i,j} + a_{i+1,j}\phi_{i+1,j} + a_{i,j-1}\phi_{i,j-1} = 0 \qquad (17)$$

Five coefficients shown in Eq. (17) are summarized as below:

$$a_{i,j-1} = a_{i-1,j} = a_{i+1,j} = a_{i,j+1} = \frac{-1}{e^{\lambda_1 h} + e^{\lambda_2 h} - 2} \qquad (18a)$$

$$a_{i,j} = \frac{e^{\lambda_1 h} + e^{\lambda_2 h} + 2}{e^{\lambda_1 h} + e^{\lambda_2 h} - 2} \qquad (18b)$$

Expanding $\phi_{i,j-1}$, $\phi_{i-1,j}$, $\phi_{i+1,j}$, and $\phi_{i,j+1}$ in a Taylor series with respect to $\phi_{i,j}$ and substituting them into Eq. (17), after some algebra the modified equation [4] for Eq. (5) is derived as

$$\phi_{xx} + \phi_{yy} - K^2\phi = c_1(\phi_{xx} + \phi_{yy}) + c_2(\phi_{xxxx} + \phi_{yyyy}) + \text{H.O.T.} \qquad (19)$$

where

$$c_1 = -a_0 \cdot \frac{h^2}{2!} + 1 \qquad (20a)$$

$$c_2 = -a_0 \cdot \frac{h^4}{4!} \qquad (20b)$$

$$a_0 = \frac{2K^2}{e^{Kh} + e^{-Kh} - 2} \qquad (20c)$$

and H.O.T. is higher-order terms. By applying L'Hôpital's rule twice, we can have

$$\lim_{h\to 0} c_1 = \lim_{h\to 0}\left(\frac{-K^2 h^2}{e^{Kh} + e^{-Kh} - 2}\right) + 1 = \lim_{h\to 0}\left(\frac{-2K^2 h}{Ke^{Kh} - Ke^{-Kh}}\right) + 1$$

$$= \lim_{h\to 0}\left(\frac{-2K^2}{K^2 e^{Kh} + K^2 e^{-Kh}}\right) + 1 = 0$$

Therefore, the analytic solution can be obtained as the grid size approaches zero, implying the satisfaction of the scheme consistency.

## 5.  VALIDATION STUDY

As is normally the case when a new scheme for solving the differential equation is presented, we have to validate the proposed scheme. For this reason, we will employ test problems which are amenable to analytic solutions. We begin by validating the Helmholtz equation and then the convection-diffusion equation. Both one- and two-dimensional problems are investigated.

## 5.1   Validation of the Helmholtz Equation

To illustrate the applicability of the proceeding one-dimensional scheme for the Helmholtz equation, we consider a stringent test problem given below:

$$\phi_{xx} - k^2\phi = gl\delta(x - \eta) \tag{21}$$

In the above, $\delta$ is the delta function. As for $\eta$, its value ranges between $-l$ and $l$. Subject to the boundary conditions $\phi(l) = \phi(-l) = 0$, the solution to Eq. (21) can be derived analytically as

$$\phi(x, k, \eta) = \begin{cases} -\dfrac{gl}{k} \dfrac{\sinh[k(l - \eta)]}{\sinh(2kl)} \sinh[k(x + l)] & -l < x < \eta \\[4mm] -\dfrac{gl}{k} \dfrac{\sinh[k(l + \eta)]}{\sinh(2kl)} \sinh[k(l - x)] & \eta < x < l \end{cases} \tag{22}$$

The proof is detailed in the Appendix. The solution is computed at the chosen values of $\eta = 0$, $l = 1$, $g = 1,000$, and $k = 113$. For the case with uniform grid size $h = 10^{-3}$, it is found from Figure 1 that the finite-difference solution reproduces the analytic solution of the test equation. The values of $h$ and $k$ are chosen in order to demonstrate the ability of the present scheme to capture the sharp profile of $\phi$
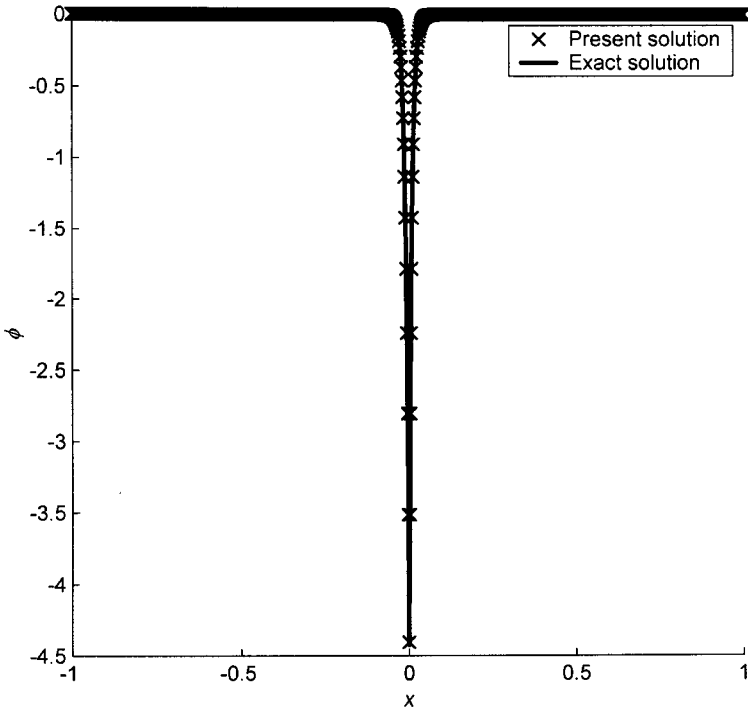


**Figure 1.** A comparison of numerical solution with that of the exact solution given in Eq. (22).

The theory showing that the present scheme can compute nonoscillatory profiles is known as the M-matrix theory. Considering the one-dimensional scheme $a_{i-1}\phi_{i-1} + a_i\phi_i + a_{i+1}\phi_{i+1} = f_i$, the coefficients given in Eq. (15) are featured by having the properties: (i) $a_i > 0$, $a_{i+1} < 0$ and $a_{i-1} < 0$; (ii) $|a_i| > |a_{i-1}| + |a_{i+1}|$. These conditions are unconditionally satisfied, implying that the matrix $[a_i]$ in $\sum a_i\phi_i = f$ is classified as being an M-matrix [5, 6]. The construction of the tri-diagonal M-matrix explains why solution profiles can be well captured without showing ripples.

Simulations were also performed in the two-dimensional domain. In this article, we justify the use of the proposed ADI scheme to simulate the following equation in the square $0 \leq x, y \leq \pi$:

$$\phi_{xx} + \phi_{yy} + \phi = 0 \tag{23}$$

The above equation, subject to the Dirichlet-type boundary condition for $\phi$, is amenable to the following exact solution [7]:

$$\phi = \cos y - \frac{\sqrt{2}}{2}\sin\left(\frac{\pi}{4}+y\right)\left[C\left(\sqrt{\frac{2(\rho - y)}{\pi}}\right) + S\left(\sqrt{\frac{2(\rho + y)}{\pi}}\right)\right]$$
$$- \frac{\sqrt{2}}{2}\sin\left(\frac{\pi}{4}-y\right)\left[C\left(\sqrt{\frac{2(\rho + y)}{\pi}}\right) + S\left(\sqrt{\frac{2(\rho - y)}{\pi}}\right)\right] \tag{24}$$

In the above, $S(\cdot)$ and $C(\cdot)$ denote the Fresnel sine integral and Fresnel cosine integral, respectively.

As Figure 2 shows, the solution computed at $h = \pi/20$ agrees well with the exact solution. We also carried out computations on continuously refined grids, namely, $h = \pi/10$, $\pi/20$, $\pi/40$, $\pi/60$, and $\pi/80$, and computed the prediction errors in their $L_2$ norms. This was followed by plotting $\log(\mathrm{err}_1/\mathrm{err}_2)$ against $\log(h_1/h_2)$ for the errors $\mathrm{err}_1$ and $\mathrm{err}_2$ computed at two continuously refined grids $h_1$ and $h_2$. As Figure 3 shows, the rate of convergence is obtained as 1.91 using the proposed scheme.

## 5.2. Validation of the Convection-Diffusion Equation

Having validated the scheme for solving the Helmholtz equation, we apply this scheme together with the mapping given in Eq. (4) to compute the convection-diffusion equation. In the first place, we consider the following equation in $0 \leq x \leq 1$:

$$\Phi_x - \nu\Phi_{xx} = 0 \tag{25}$$

This equation is amenable to the following solution [8]:

$$\Phi(x) = \frac{1 - e^{-[(1-x/\nu)]}}{1 - e^{-1/\nu}} \tag{26}$$

For the case with a uniform grid size $h = 1/200$, the computed result shown in Figure 4 is found to reproduce the analytic solution of the test equation. This test verifies that the proposed finite-difference scheme can provide a nodally exact steady-state solution. At $\nu$ continuously decreases (say, $\nu = 7\times10^{-4}$), the prediction
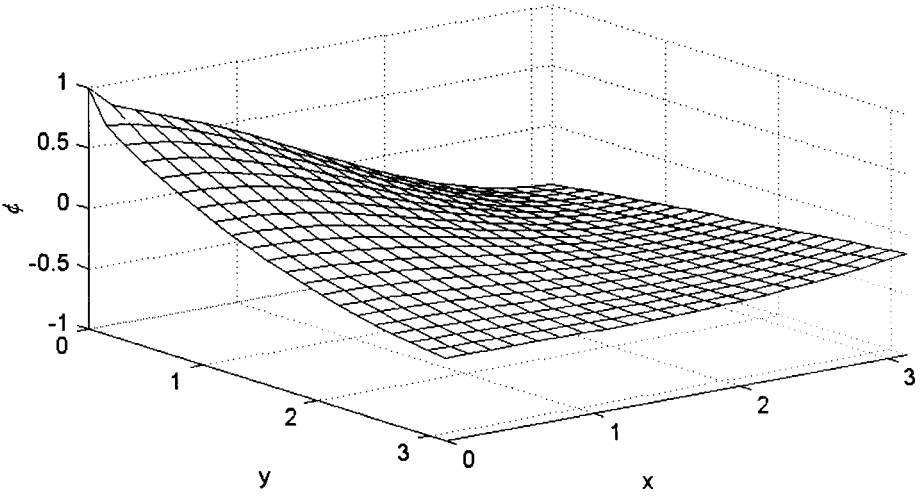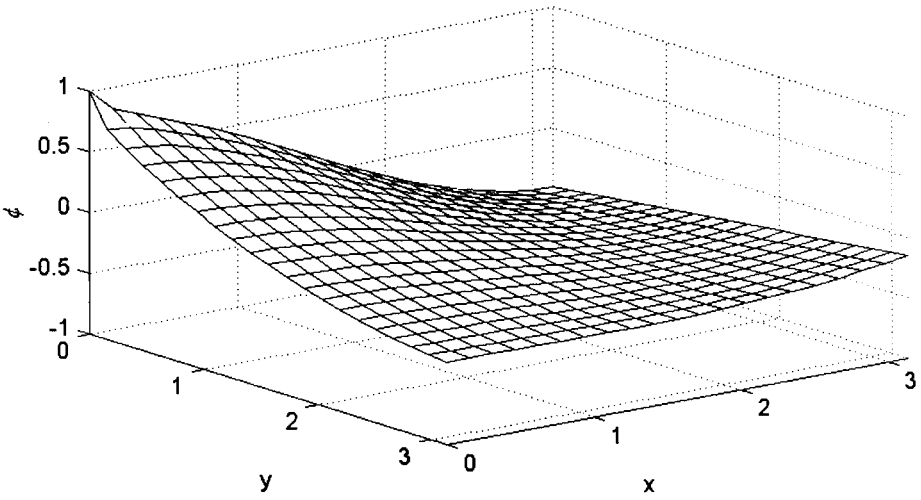
**Figure 2.** A comparison of finite-difference and exact solutions: (*a*) exact solution given in Eq. (24); (*b*) present solution.
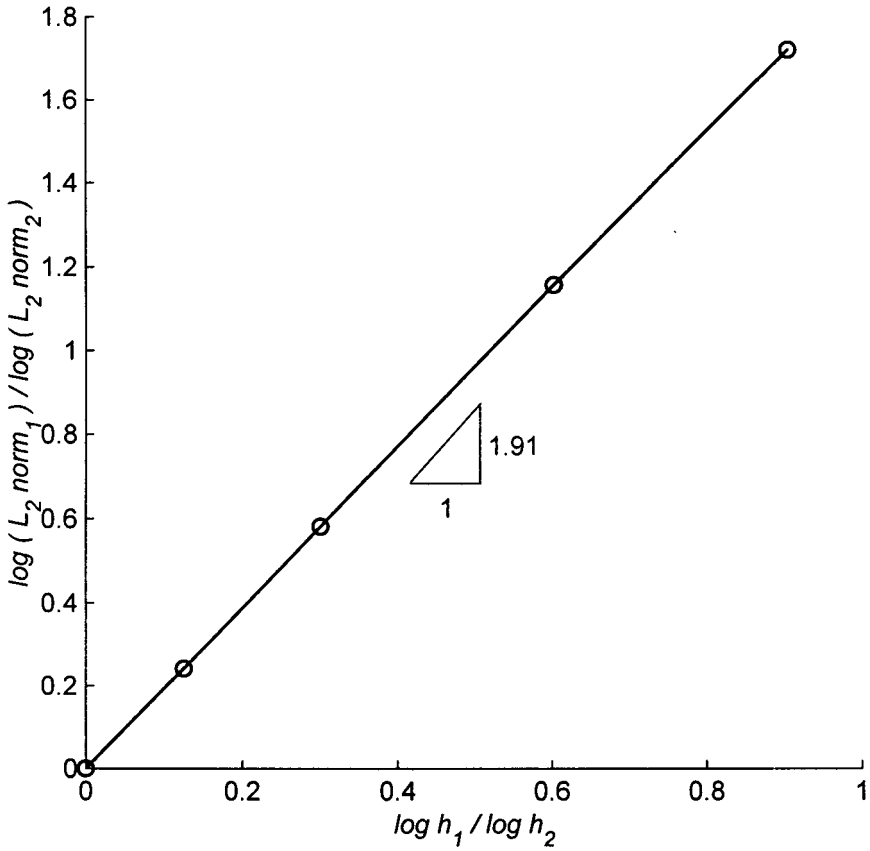
**Figure 3.** The rate of convergence using the proposed finite-difference scheme for solving Eq. (23).

accuracy deteriorates due to errors arising from the calculation of Eq. (4). Such an error is due solely to the machine error and has nothing to do with the method itself. The effort to resolve this difficulty is currently under investigation so that we can develop the scheme for use in practical situations.

Having validated the code against the above one-dimensional test problem, our attention is now drawn to the two-dimensional convection-diffusion equation. As noted previously, we have to provide evidence when validating the scheme. For this reason, we solve for the following equation, which is amenable to the following analytical solution in $0 \leq x, y \leq 1$:

$$\frac{\bar{a}}{\mu}\Phi_x + \frac{\bar{b}}{\mu}\Phi_y = \Phi_{xx} + \Phi_{yy} \qquad (27)$$

For simplicity, $\bar{a}$ and $\bar{b}$ are assumed to be constant along the $x$ and $y$ directions respectively. Subject to the Dirichlet-type boundary condition shown schematically in Figure 5, the exact solution to the above linearized viscous Burgers equation (27)
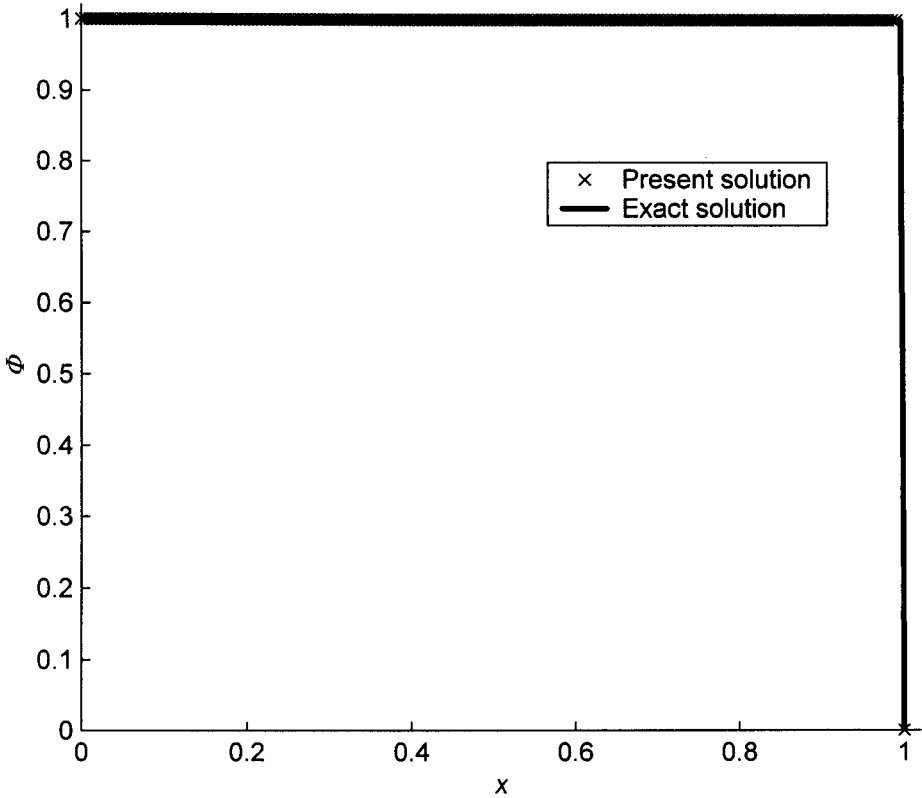
**Figure 4.** A comparison of the numerical solution and the exact solution given in Eq. (26).

is given by [9]:

$$\Phi(x, y) = \left\{\frac{1 - \exp[(x - 1)(\bar{a}/\mu)]}{1 - \exp(-\bar{a}/\mu)}\right\} \left\{\frac{1 - \exp[(y - 1)(\bar{b}/\mu)]}{1 - \exp(-\bar{b}/\mu)}\right\} \qquad (28)$$

Following the methodology just described, we first solve the Helmholtz equation (5) for $\phi$. The coefficient $K^2$ for this test is $K^2 = (\bar{a}^2 + \bar{b}^2)/4\mu^2$. Computations at $\mu = 1$ have been carried out at five mesh sizes, namely, $h = 1/8, 1/16, 1/32, 1/64$, and $1/128$. Upon obtaining the corresponding solutions $\phi$ from the Helmholtz equation, we can compute solutions $\Phi$ at five investigated grids according to the mapping given in Eq. (4), yielding

$$\Phi = e^{(\bar{a}/2\mu)x + (\bar{b}/2\mu)y} \phi(x, y) \qquad (29)$$

For each case, the computed error is cast in its $L_2$ error norm. This is followed by plotting $\log(\text{err}_1/\text{err}_2)$ against $\log(h_1/h_2)$ for errors $\text{err}_1$ and $\text{err}_2$, which are computed at two consecutively refined meshes $h = h_1$ and $h = h_2$. With these error norms, the rate of convergence of the proposed scheme is obtained and is plotted in Figure 6
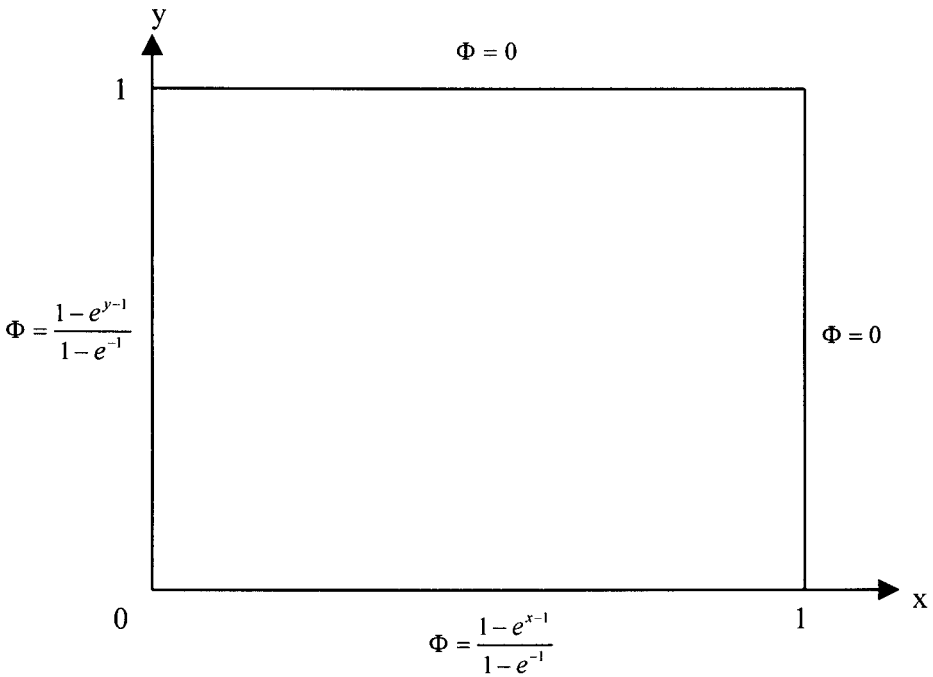
**Figure 5.** A schematic of the test problem, given by Eqs. (27)–(28), in a unit square.

for the sake of clarity. Good agreement with the results, as shown in Figure 7, and fast convergence to the analytic solution are demonstrated.

This is followed by considering Eq. (1) which involves the variable velocity field given by $(u, v) = (e^y, 0)$. Under the circumstances that $k = 1$ and $\Gamma = 0$, the exact solution is derived as $\Phi_{\text{exact}} = e^y$. The derivatives $\Phi_x$ and $\Phi_y$ shown on the right-hand side of Eq. (5) are approximated by the centered scheme using the most updated value of $\Phi$. Upon obtaining the coefficients $K^2, \bar{f}, C$, and $D$, we can apply the proposed finite-difference scheme. The iterative calculation procedures continue until the difference in $\phi$ between two consecutive iterations falls below the user-specified tolerance. Following the iterative procedures, the solutions computed in the square $-1 \leq x \leq 1, 0 \leq y \leq 1$ can be shown in Figure 8. The computed error cast in its $L_2$ norm is obtained as $4.4576 \times 10^{-4}$ for the case involving the uniform grid size $\Delta x = \Delta y = 1/23$.

With reasonable confidence in applying the presently developed finite-difference scheme in solving the convection-diffusion equation in two dimensions, we will next consider a much more stringent skew advection problem. This case, subject to boundary conditions, is shown schematically in Figure 9. This problem is investigated because it allows us to benchmark the scheme's ability to capture the interior layer. In the square domain $0 \leq x, y \leq 1$, we can run code at different flow angles $\theta = \tan^{-1}(\bar{b}/\bar{a}) = 12.25°, 22.5°$, and $45°$, where $|\bar{a}^2 + \bar{b}^2| = 1$. The fluid viscosity is considered to be $\mu = 3 \times 10^{-2}$. Grids are uniformly overlaid on the domain
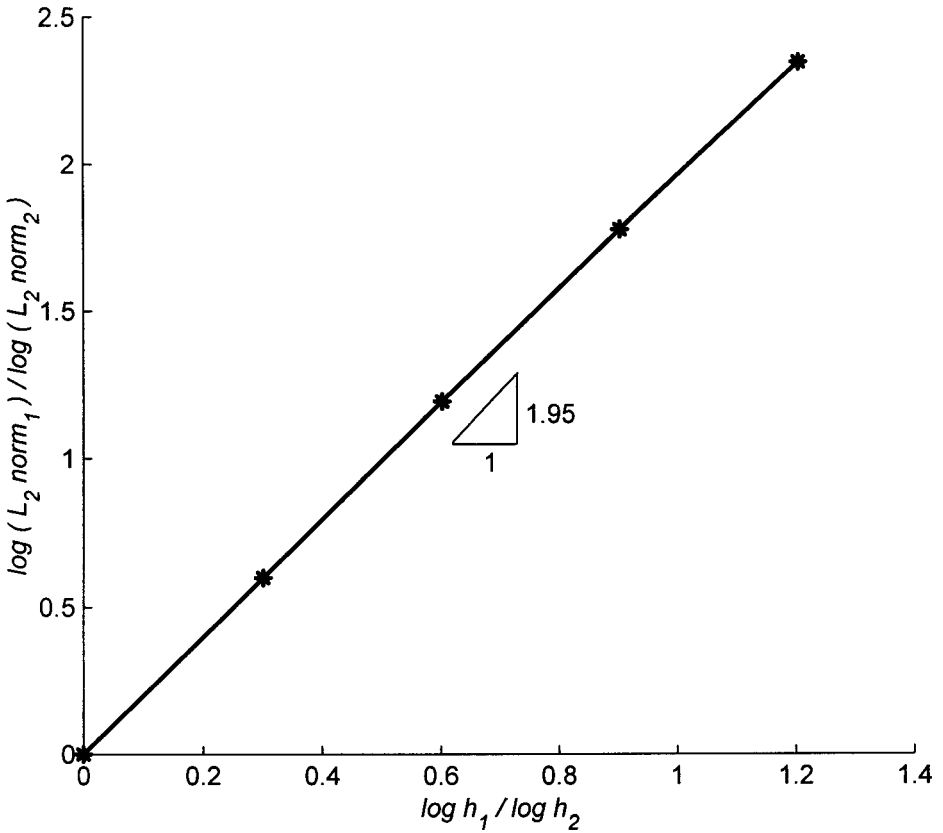
**Figure 6.** The rate of convergence for the two-dimensional convection-diffusion equation with analytic solution given in Eq. (28) using the present finite-difference scheme.

of interest and the results are plotted in Figure 10. As Figure 11 shows, all results plotted along the line $\overline{BD}$ reveal a marked change of $\Phi$ across their respective dividing line, thus demonstrating the applicability of the proposed scheme to capture steep solution in the flow interior.

## 6. CONCLUDING REMARKS

The aim of this numerical study is to tackle the convective instability in the two-dimensional simulation of convection-diffusion transport equation. Our underlying strategy is to introduce a new variable, which has a direct relevance to the passive scalar via the proposed transformation. The choice of the mapping relation shows its merit in that the equation under investigation is a Helmholtz equation. No convective terms are invoked, thereby completely overcoming the difficulty related to convective instabilities. With the transformation being applied, the key to success in predicting the convection-diffusion equation lies in the scheme quality of solving the Helmholtz equation. As effective as the scheme may provide,
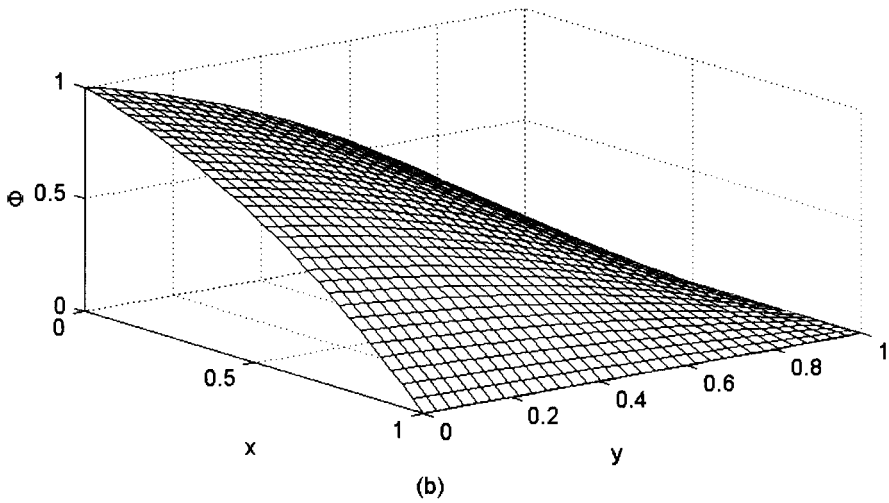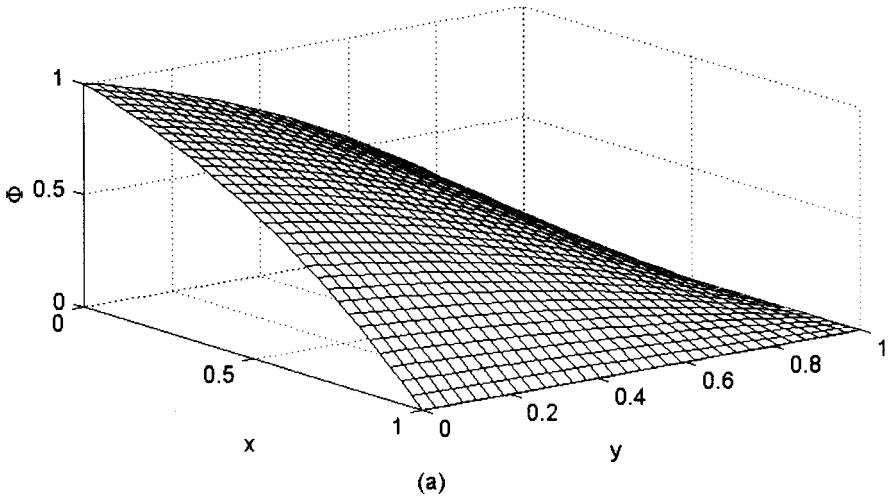
**Figure 7.** A comparison of the numerical solution and the analytic solution given in Eq. (28) for the case with $\mu = 1$: (a) exact solution; (b) present solution.
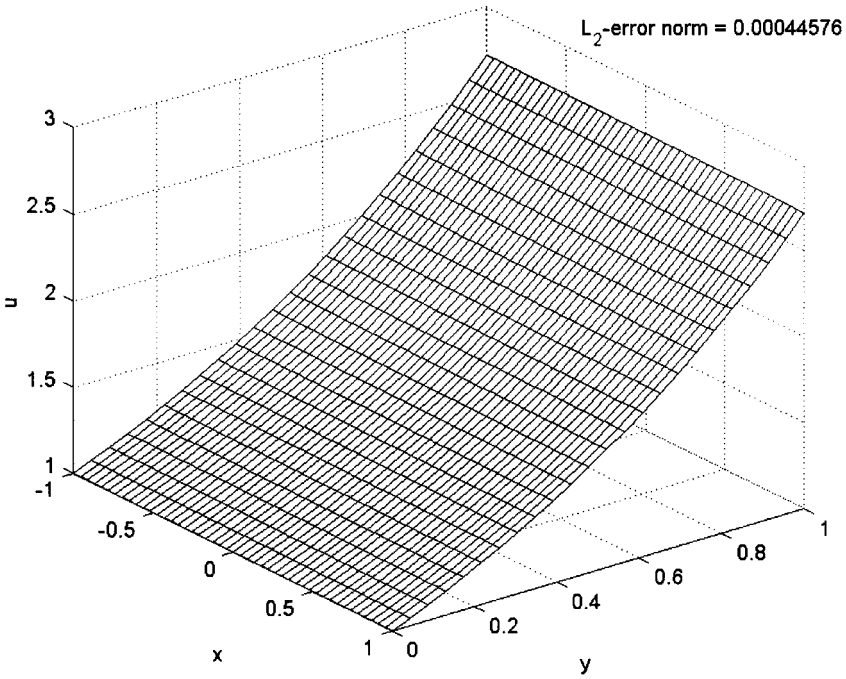
**Figure 8.** The computed solution $\Phi$ for the two-dimensional variable case considered in Section 5.2.
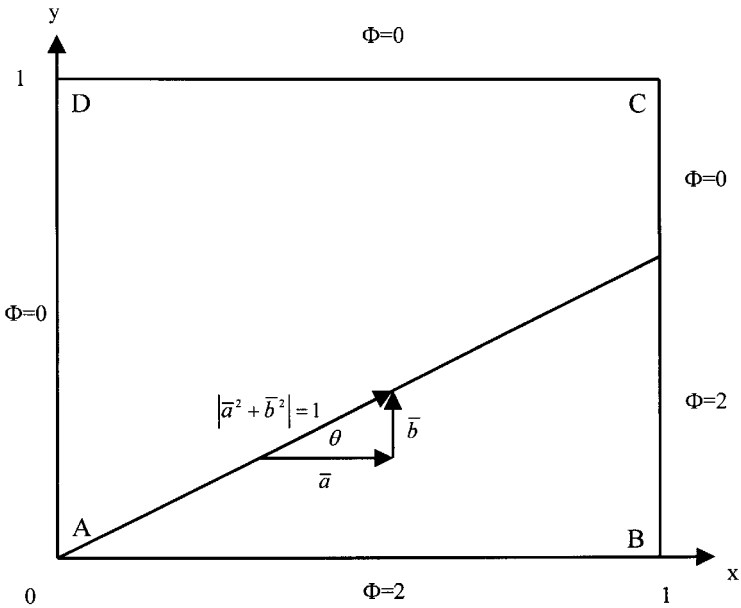


**Figure 9.** A schematic of the two-dimensional test problem for showing the ability of the proposed scheme to resolve interior sharp layer.
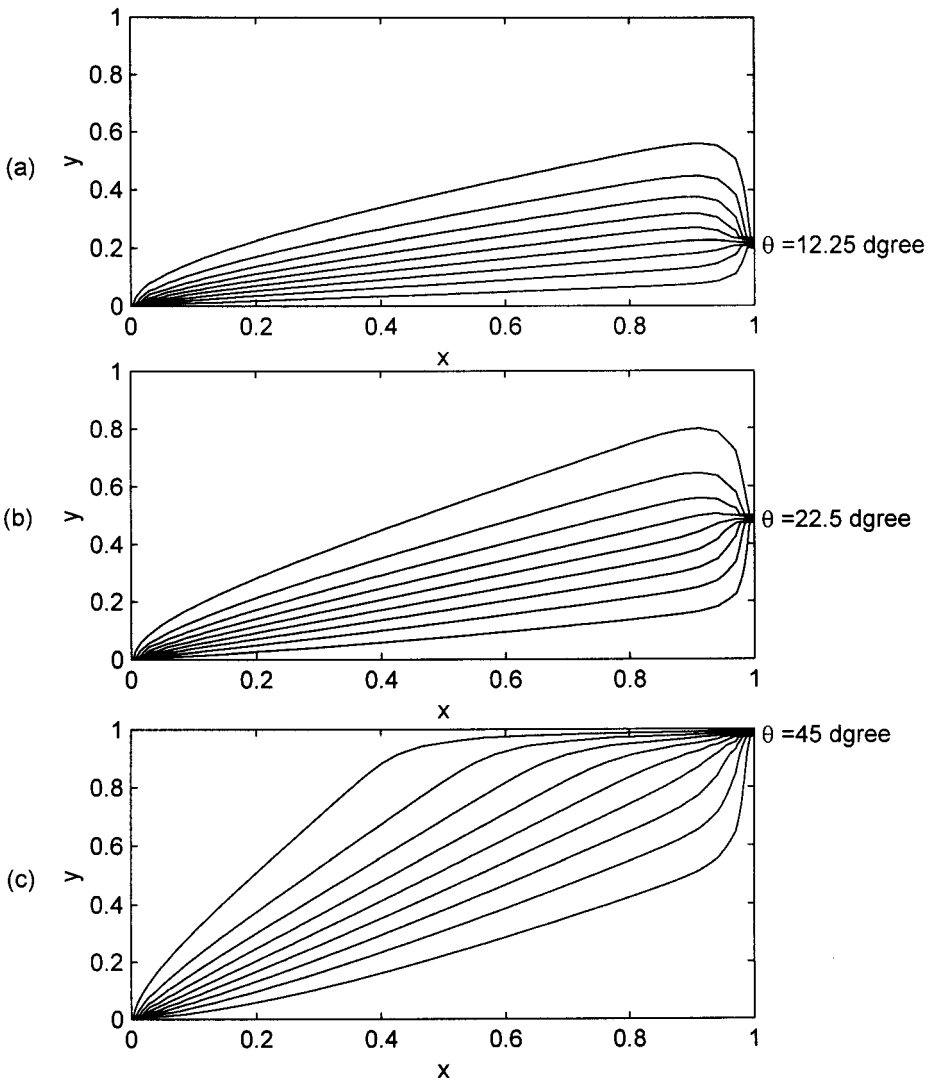
**Figure 10.** The computed contours of $\Phi$ for the investigated skew advection problem: (*a*) $\theta = 12.25°$; (*b*) $\theta = 22.5°$; (*c*) $\theta = 45°$.
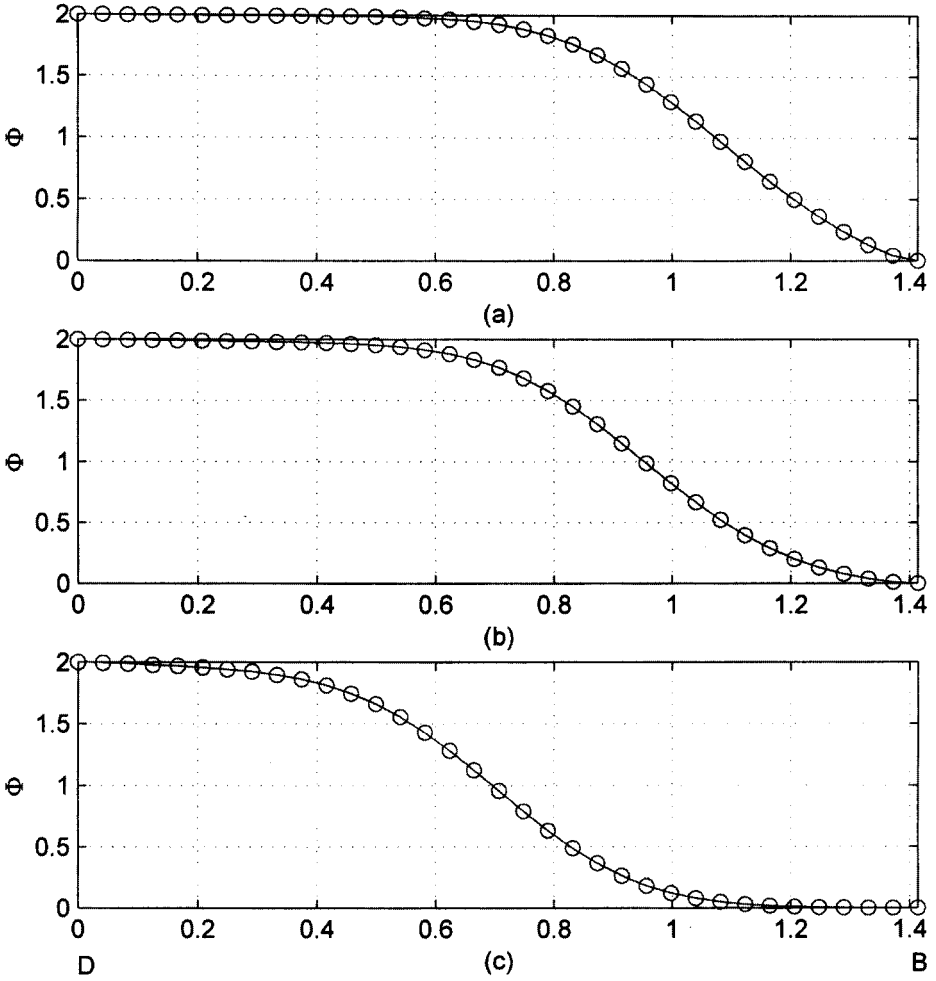
**Figure 11.** The distributions of $\Phi$ along the line $\overline{BD}$: (a) $\theta = 12.25°$; (b) $\theta = 22.5°$; (c) $\theta = 45°$.

we have considered the alternating direction implicit scheme of Polezhaev. For the sake of accuracy, we have developed a nodally exact flux discretization scheme for the one-dimensional Helmholtz equation. To elucidate the nature of the proposed scheme, we have performed modified equation analysis. A full assessment of the proposed scheme requires a rigorous test of the numerical method. For this reason, we consider problems that exact solutions to the investigated model equation are feasible. The computed $L_2$ error norms and their resulting rates of convergence validate the applicability of the two-step finite-difference advection-diffusion scheme to smooth flow analysis. For the sake of completeness, computations have been performed for a problem with a high gradient solution. Good ability to capture the sharply varying profile has been demonstrated.

## REFERENCES

1. T. J. R. Hughes and A. N. Brooks, A Multi-Dimensional Upwind Scheme with No Crosswind Diffusion, in T. J. R. Hughes (ed), *Finite Element Methods for Convection Dominated Flows*, AMD vol. 34, pp. 19–35, ASME, New York, 1979.

2. V. I. Polezhaev, Numerical Solution of the System of Two-Dimensional Unsteady Navier-Stokes Equations for a Compressible Gas in a Closed Region, *Fluid Dynamics*, vol. 2, pp. 70–74, 1967.

3. C. Pozrikidis, *Introduction to Theoretical and Computational Fluid Dynamics*, Oxford University Press, New York, 1997.

4. R. F. Warming and B. J. Hyette, The Modified Equation Approach to the Stability and Accuracy Analysis of Finite-Difference Methods, *J. Comput. Phys.*, vol. 14, pp. 159–179, 1974.

5. T. Meis and U. Marcowitz, Numerical Solution of Partial Differential Equations, in *Applied Mathematical Science*, *Vol. 32*, Springer-Verlag, Berlin, 1981.

6. T. Ikeda, Maximal Principle in Finite Element Models for Convection-Diffusion Phenomena, in *Lecture Notes in Numerical and Applied Analysis, Vol. 4*, North-Holland, Amsterdam, 1983.

7. Xiping Yu, Finite Difference Methods for the Reduced Water Wave Equation, *Comput. Meth. Appl. Mech. Eng.*, vol. 154, pp. 265–280, 1998.

8. Saul Abarbanel and Adi Ditkowski, Multi-dimensional Asymptotically Stable Finite Difference Schemes for the Advection-Diffusion Equation, *Comput. Fluids*, vol. 28, pp. 481–510, 1999.

9. J. C. Tannehill, D. A. Anderson, and R. H. Pletcher, *Computational Fluid Mechanics and Heat Transfer*, 2d ed., Taylor & Francis, London, UK, 1997.

## APPENDIX

By definition, the inhomogeneous linear Helmholtz equation (21) is mathematically equivalent to

$$
\begin{cases}
\phi_{xx} - k^2\phi = 0 \qquad -l \le x < \eta^-, \eta^+ < x \le l & \text{(A1)} \\
\phi(-l) = \phi(l) = 0 & \text{(A2)}
\end{cases}
$$

The general solution of Eq. (A1) is as follows:

$$
\phi = \begin{cases}
Ae^{kx} + Be^{-kx} \qquad -l \le x \le \eta^- & \text{(A3a)} \\
Ce^{kx} + De^{-kx} \qquad \eta^+ \le x \le l. & \text{(A3b)}
\end{cases}
$$

Four equations are needed to determine four undetermined parameters $A$, $B$, $C$, $D$.

Substituting the boundary conditions $\phi(-l)=0$ and $\phi(l)=0$ into Eqs. (A3a) and (A3b), we get, respectively,

$$
Ae^{-kl} + Be^{kl} = 0 \tag{A4}
$$

and

$$
Ce^{kl} + De^{-kl} = 0 \tag{A5}
$$

Derivation of the third and fourth equations is followed by integrating Eq. (A1), resulting in $\int_{\eta^-}^{\eta^+} \phi_{xx}dx - k^2 \int_{\eta^-}^{\eta^+} \phi dx = gl \int_{\eta^-}^{\eta^+} \delta(x - \eta)$. By virtue of the mathematical identity $\int_{\eta^-}^{\eta^+} \delta(x - \eta) = 1$, we have

$$
\phi_x|_{\eta^-}^{\eta^+} - k^2\phi(\eta)(\eta^+ - \eta^-) = gl \tag{A6}
$$

Let $\phi$ be continuous at $x=\eta$; this continuity condition at $x=\eta$ demands that

$$
Ae^{k\eta} + Be^{-k\eta} = Ce^{k\eta} + De^{-k\eta} \tag{A7}
$$

Under the continuity condition of $\phi$ at $x=\eta$, Eq. (A6) turns out to be

$$
\phi_x|_{x=\eta^+} - \phi_x|_{x=\eta^-} = gl \tag{A8}
$$

By taking derivatives of the two equations given in (A3) and substituting them into Eq. (A7), we get

$$
Cke^{k\eta} - Dke^{-k\eta} - Ake^{k\eta} + Bke^{-k\eta} = gl \tag{A9}
$$

After some algebra, four coefficients $A$, $B$, $C$, and $D$ can be uniquely solved using

Eqs. (A4), (A5), (A7), and (A9):

$$A = \frac{-gle^{kl} \sinh[k(l - \eta)]}{2k \sinh(2kl)}$$

$$B = \frac{gle^{-kl} \sinh[k(l - \eta)]}{2k \sinh(2kl)}$$

$$C = \frac{gle^{-kl} \sinh[k(l + \eta)]}{2k \sinh(2kl)}$$

$$D = \frac{-gle^{kl} \sinh[k(l + \eta)]}{2k \sinh(2kl)} \tag{A10}$$

The analytic solution of Eq. (21) is thus obtained as

$$\phi = \begin{cases} -\dfrac{gl \sinh[k(l - \eta)] \cdot \sinh[k(l + x)]}{k \cdot \sinh(2kl)} & -l \leq x \leq \eta^{-} \\[4mm] -\dfrac{gl \sinh[k(l + \eta)] \cdot \sinh[k(l - x)]}{k \cdot \sinh(2kl)} & \eta^{+} \leq x \leq l \end{cases} \tag{A11}$$